Florian Czeczil and Richard Pasteka*

Computational Fluid Dynamics in Preterm Neonatal Airways: Insights into Airflow Dynamics and Aerosol Deposition

Abstract: The primary cause of death in extremely prematurely born infants is acute respiratory distress syndrome (ARDS). To manage this condition, both invasive ventilation and less invasive methods like continuous positive airway pressure (CPAP) are employed. Recently, there has been growing interest in delivering aerosolized medication directly to the lungs as a non-invasive therapeutic option. However, the effectiveness of such aerosol delivery in extremely premature infants remains poorly understood due to their unique airway anatomy. To address this gap, a three-dimensional model of the upper airway geometry of an extremely prematurely born neonate was segmented from an MRI scan. This model was used to perform computational fluid dynamics (CFD). The analysis aimed to evaluate airflow behavior and aerosol deposition patterns under CPAP ventilation conditions. The results demonstrate velocity and pressure contours that are consistent with previous CFD studies in adults and older infants, while revealing new quantitative insights specific to the narrow and delicate airways of extremely premature neonates. Notably, the simulations capture the presence of a laryngeal jet even at this early developmental stage. Furthermore, particle tracking analyses highlight specific regions prone to frequent aerosol deposition, which may limit the uniform delivery of inhaled medication to the lower lungs. These findings suggest that CFD modeling can play a crucial role in optimizing aerosolbased therapies for this vulnerable population. Further work is needed to validate the results against in-vitro experiments and to expand the model to include the oral cavity, enabling future investigation of oral inhalation strategies.

Keywords: Computational fluid dynamics, Preterm neonates, Upper airways, Simulation, Aerosol deposition

1 Introduction

Acute respiratory distress syndrome (ARDS) remains a primary cause of morbidity and mortality in extremely premature infants. Due to the underdeveloped nature of their lungs and

Florian Czeczil, University of Applied Sciences Technikum Wien, Vienna, Austria, e-mail: florian.czeczil@technikum-wien.at *Corresponding author: Richard Pasteka, University of Applied Sciences Technikum Wien, Vienna, Austria, e-mail: pasteka@technikum-wien.at

airways, these infants are highly susceptible to severe respiratory complications. While invasive ventilation has been the standard care for long, less invasive methods such as high-frequency oscillator ventilation and continuous positive airway pressure (CPAP) have emerged as promising alternatives, reducing the risk of ventilation-induced lung injury. However, CPAP is indicated only when the preterm neonate is spontaneously breathing. [6, 7] In parallel, the targeted delivery of aerosolized medications, such as surfactant therapies and other inhalable drugs, could further improve respiratory outcomes by directly addressing pulmonary diseases. Although neonates can sustain spontaneous oral breathing in situations of nasal occlusion, they are predominantly nasal breathers [3, 9], which further underscores the importance of understanding nasal airflow dynamics and aerosol deposition patterns in this population.

Previous research employing computational fluid dynamics (CFD) to analyze neonatal airflow patterns has primarily focused on comparing infant airflow dynamics to those of adults [3], investigating the impact of spherical and anatomically designed masks on airflow and wall stress in neonatal upper airways during resuscitation [4], examining airflow dynamics as well as the deposition and hygroscopic growth of PM2.5 particles in both an adult and a 5-year-old boy [12], and studying airflow characteristics including particle deposition patterns, velocity, and pressure in simplified models of children's upper airway tracts [8]. Additional work on the breathing patterns of preterm infants relied on data gathered from ventilatory support devices [10], which do not permit the finegrained visualization and analysis offered by CFD. To the best of the authors' knowledge, there has been no investigation into airflow and particle deposition mechanics in an anatomically accurate model of an extremely preterm infant, reconstructed from MRI data, using CFD.

This work aims to analyze the velocity, pressure, and particle deposition patterns occurring during nasal breathing in a preterm neonate using computational fluid dynamics (CFD) simulation with a realistic geometry obtained from a 7 Tesla MRI scan.

https://doi.org/10.1515/cdbme-2025-0207

2 Materials & Methods

2.1 Model acquisition

The three-dimensional (3D) model of the preterm neonatal upper airway geometry was acquired through segmentation of an MRI scan of a neonate at 23 weeks postmenstrual age. At this development stage, the fetus is classified as "extremely preterm" by the World Health Organization (WHO).[11]The original image data, stored in a DICOM format, was imported into 3D Slicer for model creation.

The segmentation process was performed manually by annotating the structures of interest on a slice-by-slice basis using a combination of level-tracing, paint, and drawing tools. At this stage, only the airway lumen was segmented, as it constitutes the primary domain for the subsequent computational fluid dynamics (CFD) analysis.

Following segmentation, the model was post-processed in 3-matic (Materialise NV, Leuven, Belgium). As the presence of issues in the geometry, such as holes, overlapping edges, or duplicate triangles, compromise the quality of the mesh, they had to be corrected. In addition, the geometry was gently smoothed, a uniform wall thickness of 0.5 mm was assigned, and openings were created at the nostrils and trachea to allow realistic airflow during simulations.

2.2 CFD Simulation

Airflow dynamics and particle deposition within the nasal cavity, nasopharynx, and larynx were simulated using Ansys Fluent 2024 Academic (Ansys Inc., Pennsylvania, USA). The STL files generated from the post-processed model were imported into Fluent 2024, where a computational mesh was generated to enable a stepwise numerical solution of the flow field.

Due to the small-scale geometry, featuring narrow passages and sharp bends, convergence of the simulation was achieved through a two-step approach. Initially, a steady-state simulation was performed, and convergence was achieved after approximately 200 iterations. The steady-state solution served as the initial condition for a subsequent transient simulation to capture the dynamic nature of neonatal airflow better. Afterwards, a transient simulation was performed with the settings visible in Table 1. The time step sizes and velocity magnitude parameters were calculated following the values provided in [10].

The boundary conditions for the nasal inlets velocity was calculated from the 0.2–0.3 L/min/kg average reported in [1] and the surface area of the inlets. The preterm infant analyzed in this study weighed 520 grams.

Tab. 1: Settings used for meshing and simulation in Ansys Fluent 2024

| Setting Name | Value |
|------------------------------------|--------------------------|
| Volume Mesh | |
| Fill | poly-hexcore |
| Cell Amount | 1,624,299 |
| Boundary Conditions | |
| Nasal Inlet Velocity Magnitude | 0.62 m/s |
| Trachea Outlet Gauge Pressure | 0 Pa |
| Wall DPM Condition | Trap |
| Inlet & Outlet DPM Condition | Escape |
| DPM Settings | |
| Injection Velocity Magnitude | 0.62 m/s |
| Diameter Distribution | Rosin-Rammler |
| Diameter Range | $1 \text{ to } 10 \mu m$ |
| Inject Using Face Normal Direction | On |
| Steady-State Stage | |
| Initialization | Hybrid |
| Solver | SIMPLEC |
| Transient Stage | |
| Initalization | from Steady-State |
| Time Step Size | 10^{-5} s |
| Calculation Duration | approx. 14 hrs |

The particles were injected along the normal surface vector at the inlets with an injection velocity equal to the local airflow velocity, with a simultaneous injection (0 s injection time) to mimic the initial phase of aerosol administration.

Finally, cross-sectional planes were created along the entire geometry and labeled with letters from A to V. The finished model obtained after post-processing, including the planes selected for visualization of contours and calculation of particle deposition in the airways, Figure 1.

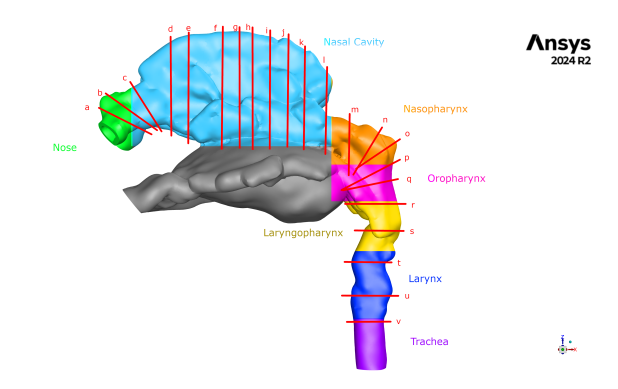


Fig. 1: 3D model obtained from MRI segmentation depicting key anatomical structures along with the cross-sectional planes used for flow and pressure contours, and particle deposition measurements.

3 Results

The velocity profile depicted in Figure 2 shows that after initially entering the nasal cavity, the overall flow speed decreases. Slightly higher velocities are observed along the inner walls of the nasal cavity compared to the outer walls. In the nasopharynx, the flow velocity begins to increase slightly, a trend that continues through the laryngopharynx and into the larynx. The highest flow velocity occurs in the larynx.

The pressure contours extracted from the simulation, shown in Figure 3, exhibit a pattern that is inversely related to the velocity curves (Figure 2). The highest pressure is observed shortly after the air enters the nasal cavity, corresponding to the region of lowest flow velocity. As air progresses through the upper airway, pressure gradually decreases, reaching a minimum at the laryngeal jet. A slight pressure increase is then observed at the end of the larynx.

The particle deposition patterns reveal that most larger particles (> $7, \mu m$) deposit shortly after entering the nasal cavity. Subsequently, medium-sized particles (approximately $5, \mu m$) tend to deposit in the lower regions of the nasal cavity,

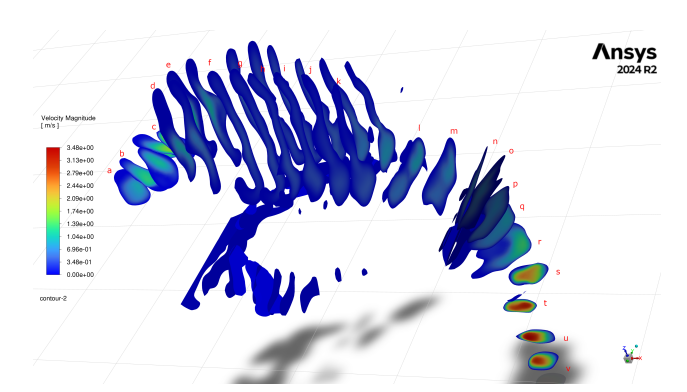


Fig. 2: Velocity distribution across various model sections, depicted by a color gradient from 0 m/s (blue) to 3.5 m/s (red).

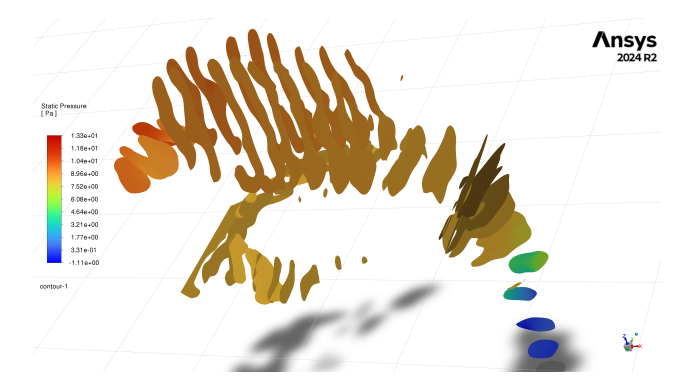


Fig. 3: Pressure contours illustrated by a gradient from 0 Pa (blue) to 13 Pa (red), highlighting the variation in pressure levels across different sections.

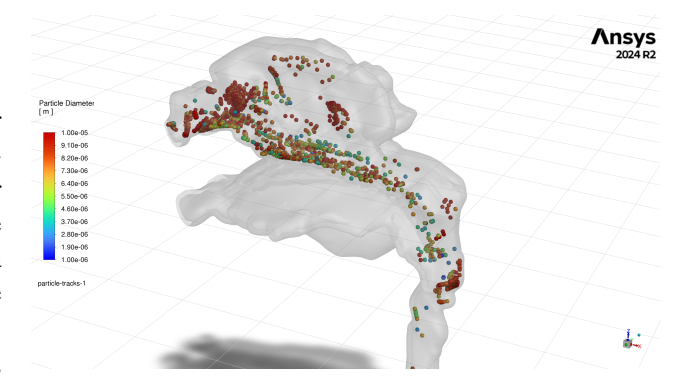


Fig. 4: Particle deposition within the neonatal airway model, depicted by a color gradient from 0 μm (blue) to 10 μm (red).

as shown in Figure 4. In the nasopharynx and laryngopharynx, particle deposition continues predominantly among mediumsized particles, with accumulation mainly on the dorsal side, particularly behind the sharp bend in the nasopharynx.

Figure 5 shows the cumulative percentage of particle deposition across the cross-sectional planes. Planes A through K span the nasal cavity, where approximately 20% of particles deposit early. In the nasopharynx, covered by planes K through O, the cumulative deposition increases by only one percentage point, indicating minimal particle loss in this region. This trend of negligible deposition continues through the laryngopharynx (planes O to S).

A significant increase in deposition is observed in the laryngeal region, between planes S and T. Here, cumulative deposition rises sharply from 21% to 37%, being the second most critical region for particle deposition in the preterm neonatal upper airways.

In the final segment of the model, the upper part of the trachea, represented by planes T through V, deposition decreases, with only a negligible increase in cumulative deposition, suggesting limited particle loss in this region.

4 Discussion

The airflow and particle deposition patterns in the upper airways of a preterm neonate were analyzed using an anatomically accurate model segmented from an MRI scan. The velocity profile shows a decrease in flow speed as air enters the nasal cavity, followed by a gradual increase through the nasopharynx and laryngopharynx, with the peak velocity occurring in the larynx. This acceleration is attributed to the constriction caused by the vocal cords, creating a laryngeal jet [2]. Conversely, the pressure contours show an inverse relationship to the velocity profile, as expected.

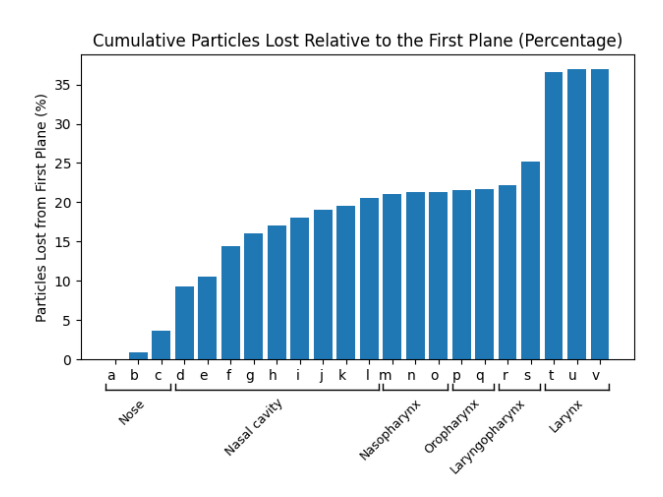


Fig. 5: Deposition of aerosol particles along observed planes in comparison to the first plane.

The velocity and pressure contours presented in Figures 2 and 3 closely resemble those reported by Corda et al. [3], who conducted simulations on a model of an 11-day-old infant and compared the results to adult cases. While the absolute velocity values differ, the overall patterns remain consistent, suggesting that airflow dynamics in extremely premature neonates and 11-day-old infants follow similar trends.

The aerosol particle deposition shows that most large particles (>7, μm) deposit early in the nasal cavity due to inertial impaction. Medium-sized particles (around 5, μm) further deposit in the lower nasal cavity and on the dorsal side of the nasopharynx, particularly at sharp bends. Although minimal deposition occurs in the nasopharynx and laryngopharynx, a significant increase is seen in the laryngeal region, where cumulative deposition increases sharply by 16%. (see Figure 5). In the upper trachea, deposition is minimal, suggesting most particles have already settled upstream. The dominant particle deposition mechanism in these neonates appears to be inertial impaction, strongly influenced by the anatomical features and flow dynamics of the airway. This finding is consistent with existing literature [5].

Future research will focus on aerodynamic behavior occurring during oral inhalation, as current research suggests that neonates can sustain spontaneous oral breathing as well as nasal breathing. [3, 9] Additionally, the simulation results could be validated against in-vitro data.

Author Statement

Research funding: This research received no specific grant. Conflict of interest: Authors state no conflict of interest. Informed consent: No individuals were included in this study. Ethical approval: The research did not require ethical approval. Declaration of Generative AI and AI-assisted technologies in the writing process: The author(s) used ChatGPT 40 to im-

prove the phrasing and clarity of the text. After using this tool, the authors reviewed and edited the content as needed and take full responsibility for the publication's content.

References

- [1] Aravanan Anbu Chakkarapani, Roshan Adappa, Sanoj Karayil Mohammad Ali, Samir Gupta, Naharmal B. Soni, Louis Chicoine, and Helmut D. Hummler. "Current concepts of mechanical ventilation in neonates" – Part 1: Basics. International Journal of Pediatrics & Adolescent Medicine, 7(1):13–18. March 2020.
- [2] T. E. Corcoran and N. Chigier. Characterization of the laryngeal jet using phase Doppler interferometry. *Journal of Aerosol Medicine: The Official Journal of the International Society for Aerosols in Medicine*, 13(2):125–137, 2000.
- [3] John Valerian Corda, B Satish Shenoy, Kamarul Arifin Ahmad, Leslie Lewis, Prakashini K, S. M. Abdul Khader, and Mohammad Zuber. Nasal airflow comparison in neonates, infant and adult nasal cavities using computational fluid dynamics. *Computer Methods and Programs in Biomedicine*, 214:106538, February 2022.
- [4] John Valerian Corda, B. Satish Shenoy, Kamarul Arifin Ahmad, Leslie Lewis, K. Prakashini, Anoop Rao, S. M. Abdul Khader, and Mohammad Zuber. Computational fluid dynamics study of respiratory mask for neonatal resuscitation. Computer Methods in Biomechanics and Biomedical Engineering, pages 1–10, June 2024.
- [5] Chantal Darquenne. Deposition Mechanisms. Journal of Aerosol Medicine and Pulmonary Drug Delivery, 33(4):181– 185, August 2020.
- [6] Jenny Fraser, Moira Walls, and William McGuire. Respiratory complications of preterm birth. BMJ: British Medical Journal, 329(7472):962–965, October 2004.
- [7] Jacqueline J Ho, Prema Subramaniam, and Peter G Davis. Continuous positive airway pressure (CPAP) for respiratory distress in preterm infants. *The Cochrane Database of Sys*tematic Reviews, 2020(10):CD002271, October 2020.
- [8] Zhijian Liu, Angui Li, Xiaoxia Xu, and Ran Gao. Computational Fluid Dynamics Simulation of Airflow Patterns and Particle Deposition Characteristics in Children Upper Respiratory Tracts. Engineering Applications of Computational Fluid Mechanics, 6(4):556–571, January 2012.
- [9] Martha J. Miller, Richard J. Martin, Waldemar A. Carlo, Janie M. Fouke, Kingman P. Strohl, and Avroy A. Fanaroff. Oral breathing in newborn infants. *The Journal of Pediatrics*, 107(3):465–469, September 1985.
- [10] Arjan B Te Pas, Connie Wong, C Omar F Kamlin, Jennifer A Dawson, Colin J Morley, and Peter G Davis. Breathing Patterns in Preterm and Term Infants Immediately After Birth. *Pediatric Research*, 65(3):352–356, March 2009.
- [11] World Health Organization. Preterm birth.
- [12] Jinxiang Xi, Xiuhua A. Si, and Jong Won Kim. Characterizing Respiratory Airflow and Aerosol Condensational Growth in Children and Adults Using an Imaging-CFD Approach. In Heat Transfer and Fluid Flow in Biological Processes, pages 125–155. Elsevier, 2015.